

Using a Thermal Infrared Imager to Evaluate Mirror Temperature During Flight for THAI-SPICE

GABRIEL NORRIS

Advisor: Professor Michael Skrutskie

May 11, 2020

Department of Astronomy

University of Virginia

This thesis is submitted in partial completion

of the requirements of the

BA Astronomy Major

Using a Thermal Infrared Imager to Evaluate Mirror Temperature During Flight for THAI-SPICE

GABRIEL NORRIS¹

¹*University of Virginia Department of Astronomy*

530 McCormick Road

Charlottesville, VA 22903, USA

ABSTRACT

The purpose of this investigation is to understand the thermal behavior of the primary mirror in passively-cooled, balloon-borne telescopes by means of various temperature sensors. This study is part of a larger project for developing a high-altitude balloon for diffraction-limited IR astronomy called THAI-SPICE (Testbed for High-Acuity Imaging - Stable Photometry and Image Motion Compensation Experiment). As part of this project, a quarter-scale model of the gondola launched in October of 2019 as an experimental precursor to the full-scale flight. This gondola has temperature sensors throughout the structure, as well as a thermal imaging camera looking directly at the primary mirror. This report will focus on the processing and interpretation of this data as it relates to the primary mirror, in tandem with concurrent investigations into other areas of the thermal design, to inform future flights.

1. INTRODUCTION

THAI-SPICE (Testbed for High-Acuity Imaging - Stable Photometry and Image Motion Compensation Experiment) is a technology demonstration project that aims to enable the next generation of

balloon-borne diffraction-limited telescopes to serve as inexpensive alternatives to space telescopes. The current generation of superpressure balloons will soon enable missions of up to 100 day duration at mid-latitudes, yielding of order 1000 hours of dark observing time per flight. A diffraction-limited aperture >1 -meter in diameter could replace a significant portion of Hubble science observations and provide the photometric stability for exoplanetary transit observations competitive with missions like Kepler and TESS.

Key to achieving diffraction-limited capability is demonstrating the thermal stability and uniformity of the telescope structure and primary mirror in the complex environment of the upper stratosphere. Work by [Young et al. \(2015\)](#) showed that certain combinations of insulating materials, radiative coatings, and sun and earth shields can reduce diurnal temperature variations of a 1-m primary mirror to less than 5 Kelvin and instantaneous gradients to less than 1 K. We aim to achieve this level of control to stabilize the primary mirror temperatures without cryogenic cooling. In addition to radiation shielding, the mirror mount must be designed to limit heat transmission into the primary mirror. Along with thermal deformations of the mount affecting alignment of the optics, the mirror itself faces potential deformations due to temperature gradients. The THAI-SPICE telescope's fused silica primary mirror is 50 cm in diameter. With a thermal expansion coefficient of $5 \times 10^{-7} K^{-1}$, thermal gradients of order 1 K over 10 cm scales correspond to differential expansion of 50 nanometers or about 1/10th of the wavelength of visible light. The main goal of thermal modeling is to ensure that under flight conditions, the mirror temperature gradients would be of this order of magnitude or smaller.

2. QUARTER-SCALE EXPERIMENT

The THAI-SPICE project developed a 1/4 scale model of the THAI-SPICE gondola in order to obtain an empirical measure of thermal conditions at float altitude and ultimately determine the relative importance of radiative loading versus atmospheric coupling at various altitudes. Primarily a thermal experiment, the quarter-scale gondola included a network of 16 contact temperature sensors and a 32x24 thermal imager. This scale gondola included insulating shielding similar to the antici-

pated configuration for the full-scale gondola and carried a telescope analog, including the primary mirror, appropriately scaled.

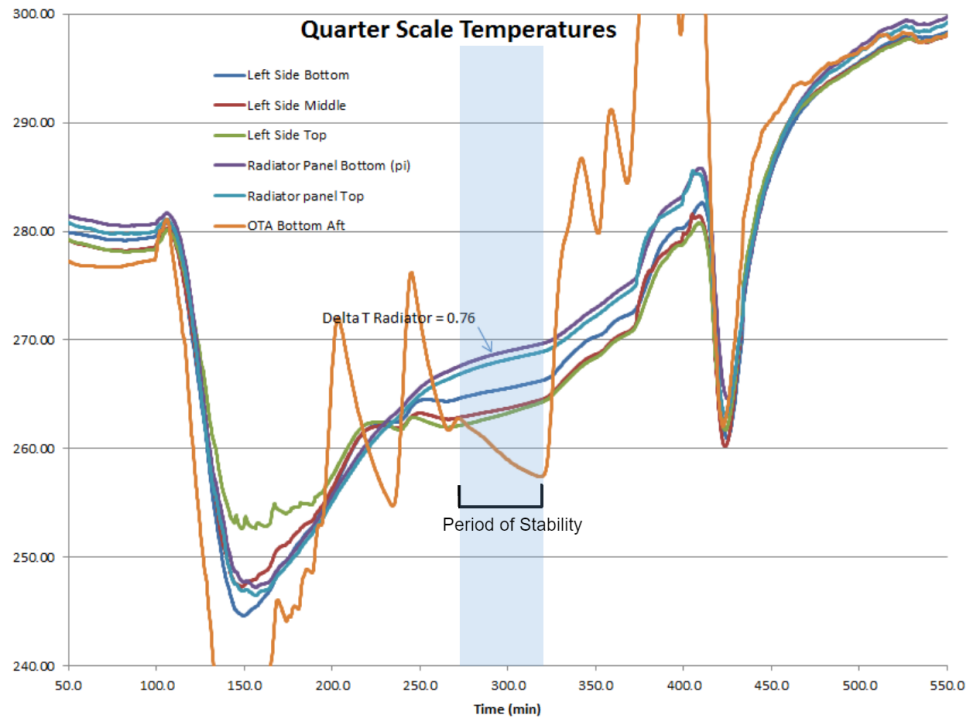


Figure 1: Full temperature profile from relevant contact sensors during the quarter-scale test flight, courtesy of Brockett (2020)

The gondola launched from the Columbia Scientific Ballooning Facility at Ft. Sumner, NM at 14:00 UTC on October 16, 2019. Launch occurred shortly after sunrise, and due to strong upper level winds the flight was terminated 5 hours later. As a result the flight took place entirely in daylight. The quarter-scale design included an azimuth control mechanism to maintain pointing of the gondola in the anti-sun direction during the daytime. This mechanism was damaged during launch and the gondola azimuth was uncontrolled during the flight as evidenced by the large temperature swings observed in the dummy telescope tube (OTA/yellow line in Fig. 1). The tube temperature reached a stable local minimum between 270 and 320 minutes of elapsed flight time indicating that, fortuitously, the gondola spent nearly an hour pointed away from the Sun. This period is highlighted in figure 1

3. LAB DATA

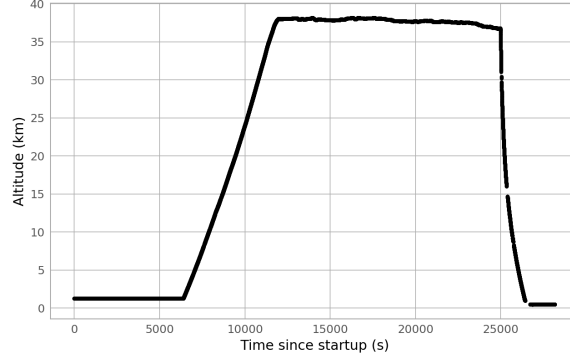


Figure 2: Altitude of the THAI-SPICE model over the course of the flight.

In order to mitigate image distortion due to differential thermal contractions, THAI-SPICE implements a passive thermal control system. Decisions about the system are informed by thermal modeling conducted in Thermal Desktop. In order to validate this simulation, a quarter-scale model of the gondola launched in October of 2019. The model had a Melexis 90640 32x24 pixel thermal imager pointed at the primary mirror recording exposures every 30 seconds.

This device is very accurate, but there is a bias pattern that emerges in the images that is more severe at lower temperatures. In order to characterize and eventually remove this bias from the images, the camera was placed in a freezer, partially insulated with polystyrene foam, and situated such that a black card filled the field-of view. The temperature was set to 20, 0, -20, -40, and -60°C , successively, and left for 30 minutes to reach equilibrium before taking 60 images over the next 30 minutes.

As can be seen in figure 4, the freezer was not able to perfectly hold temperature constant, but it was determined that the variation was low enough to continue with the flatfielding process. The mean image temperature for the whole dataset was used as the temperature for each flatfield image.

The raw mean image is the arithmetic mean of all the images taken at each data set. Two methods for removing this bias pattern were tested: multiplicative and additive correction

3.1. *Multiplicative Correction*



Figure 3: Lab Setup

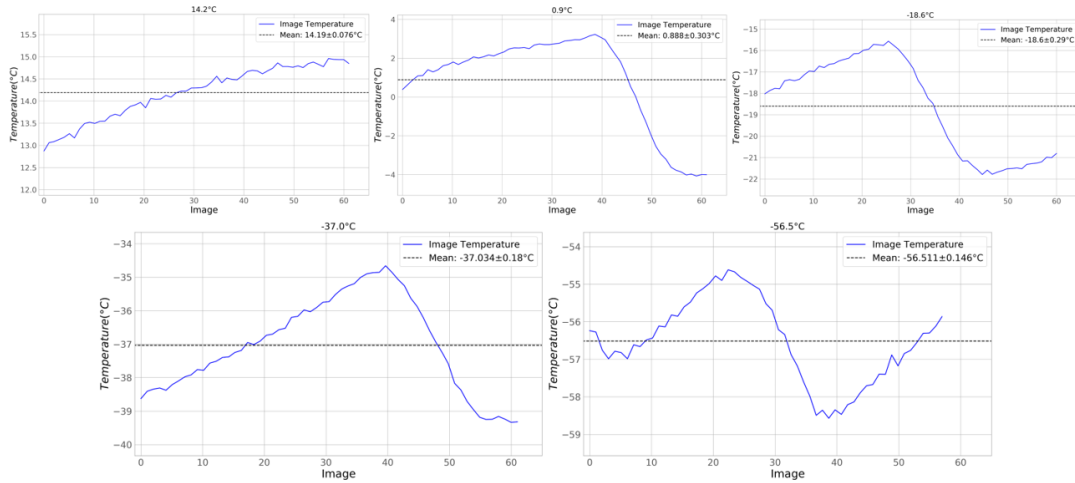


Figure 4: Average image temperature over the course of each data set.

To create the multiplicative bias frames, each raw mean image was converted from $^{\circ}C$ to $\frac{W}{m^2}$ of flux by using the Stefan-Boltzmann Law: $F = \sigma T^4$ and normalized to a mean of 1. Then, to remove this from an image, simply convert the image from temperature to flux by the same process, divide it by multiplicative bias frame corresponding to the same temperature, and convert back to $^{\circ}C$.

3.2. Additive Correction

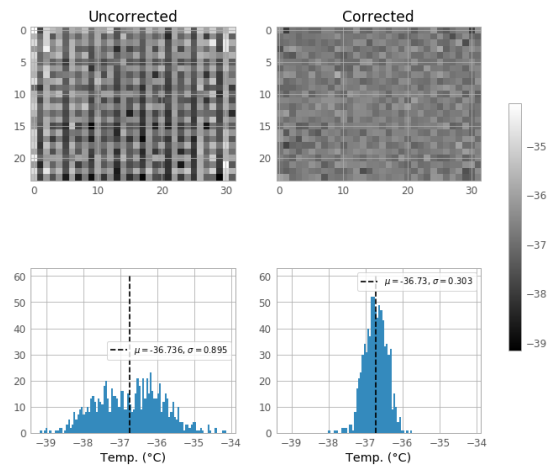


Figure 5: One typical lab image after flatfield division

To create the additive bias frames, the mean value of the frame was subtracted from each pixel, creating a matrix ranging from -2 to 2. Then, to remove this from an image, simply subtract the additive bias matrix from the image.

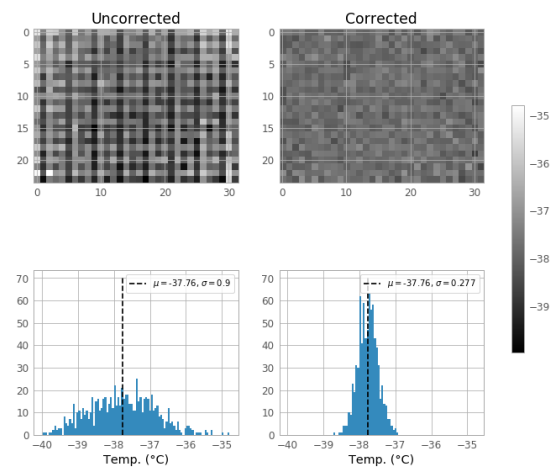


Figure 6: One typical lab image after bias subtraction

3.3. Method Comparison

As figures 5 and 6 show, both methods greatly improve the homogeneity of the lab images. Figure 7 shows that the standard deviation produced by both additive and multiplicative correction is almost exactly the same and both are a large improvement over the uncorrected images. Figure 8 shows that

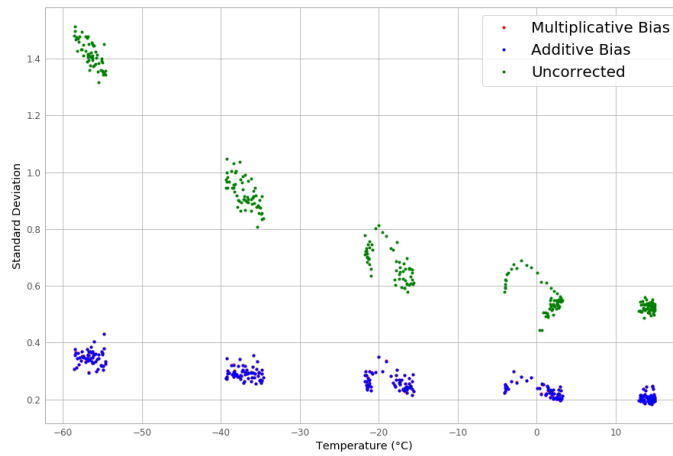


Figure 7: The standard deviation of each lab image, shown before correction as well as after both correction methods.

the difference in the means before and after correction is slightly worse for multiplicative correction, especially at lower temperatures.

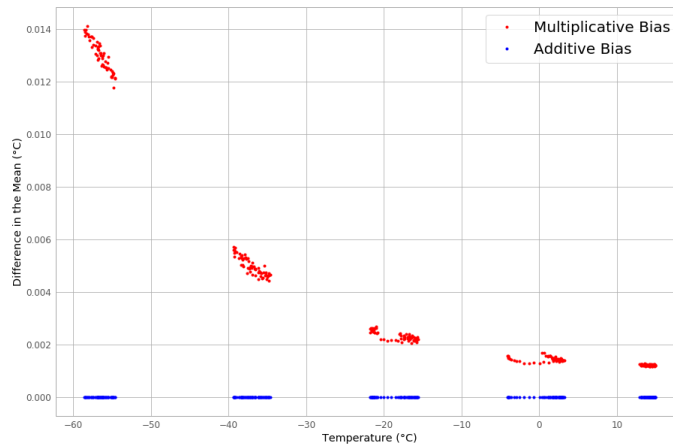


Figure 8: The difference in the mean after multiplicative and additive correction

3.4. Linear Interpolation

Since the data from the quarter-scale flight does not exactly line up with the temperature categories used in the lab setup (fig. 10), it was decided to generate new bias frames for every temperature through linear interpolation.

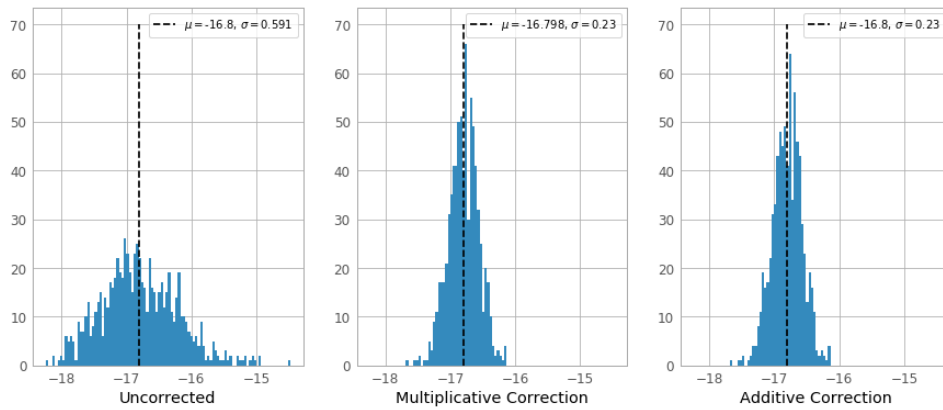


Figure 9: Histograms of one image before correction and after both corrective methods

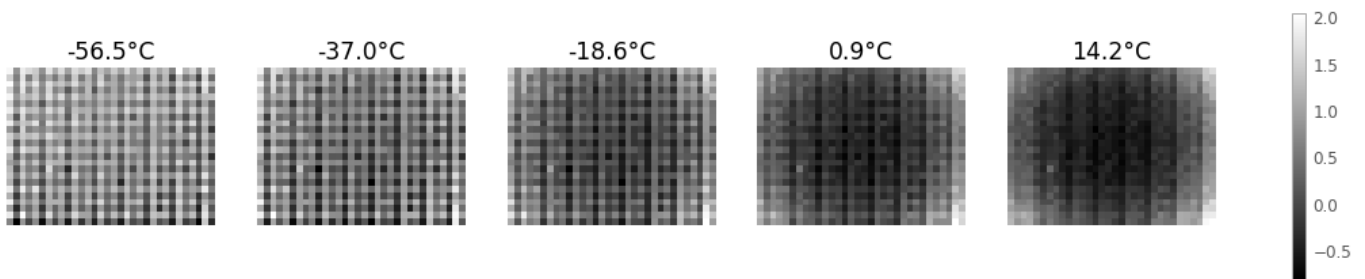


Figure 10: All additive correction frames generated from the lab data

During the quarter-scale flight, the temperature of the camera, among other health data, was logged every second. This log was used to determine the precise temperature of the device at the time each picture was taken, allowing for a new bias frame to be created for each flight image.

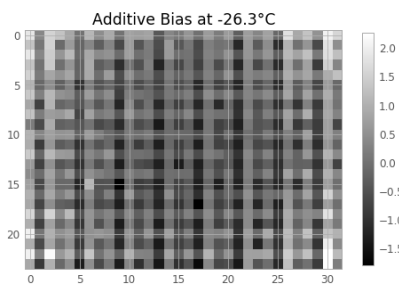


Figure 11: New bias frame generated through interpolation

4. FLIGHT DATA ANALYSIS

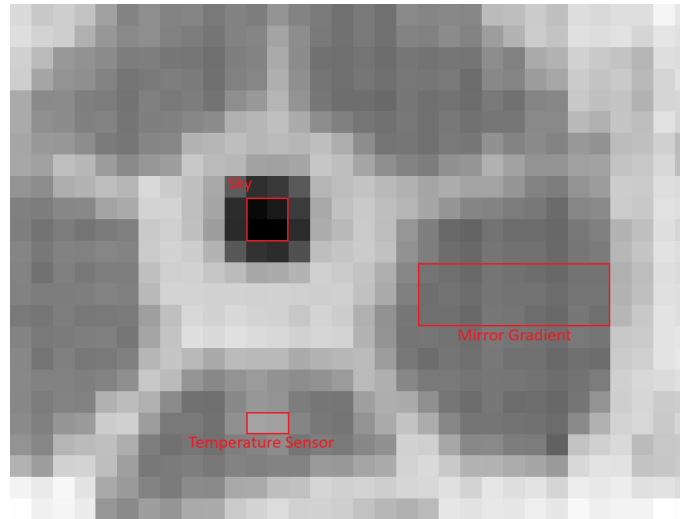


Figure 12: The average of the flight images taken during the period of stability, annotated with regions of interest. The area labeled "sky" is where the camera can see through the central hole in the primary mirror to the cold sky.

The average of each pixel in the mirror region was compared to temperature recorded by the contact temperature sensor (fig. 13). The general shape of the data reported by each sensor is very similar, meaning that the imager does a descent job reading the bulk temperature of the mirror. For all times other than ascent and descent, the thermal imager consistently reports temperatures approximately 4°C higher than the temperature sensor, and registers changes in temperature approximately 10 seconds earlier. This temperature discrepancy is likely the reflection of glow off the other warmer surfaces inside the gondola.

The source of the time discrepancy is unclear. Since the camera was on the opposite side of the mirror from the sun, one would expect its heat to reach the contact sensor first.

The radial temperature gradient in the mirror was measured (in the appropriate region from figure 12) from the center outward. The length of the measured region is 8 pixels and spans approximately 3.1 cm, for a pixel/cm ratio of 2.57. The gradient over the entire flight is shown in figure 14. The maximum gradient of $0.58^{\circ}\text{C}/\text{cm}$ occurs just before descent and the minimum gradient of $-0.76^{\circ}\text{C}/\text{cm}$ coincides with the middle of the descent. During the approximately 45 minute long

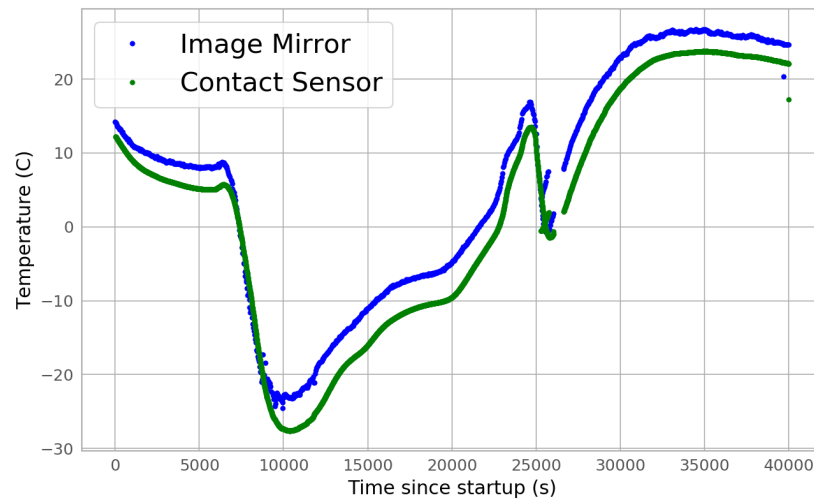


Figure 13: The mirror temperatures as measured by the thermal imager and the contact temperature sensor

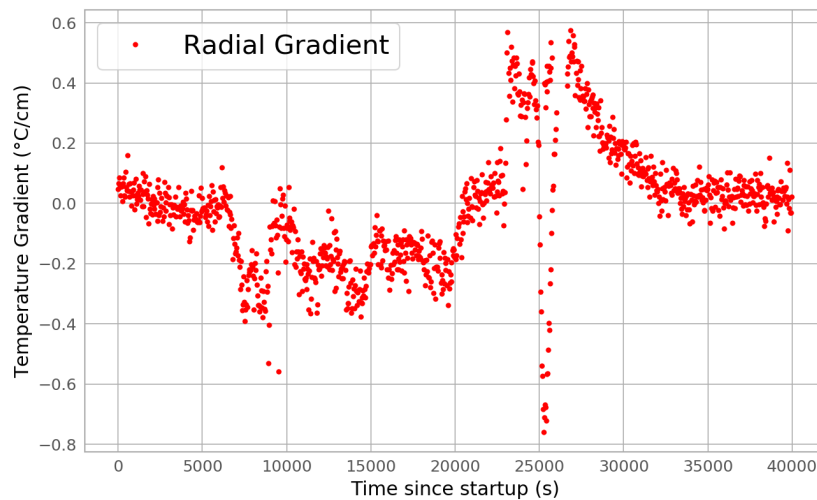


Figure 14: The radial gradient in the mirror

period of stability, the mirror held a negative temperature gradient, indicating that this was not sufficient time to reach equilibrium.

The contact temperature sensor on the inside of the far end of the telescope tube shows a nearly immediate response when the telescope faces the sun. Thus, if there is a sudden spike from that

sensor, it indicates that the sun is shining directly on and warming the mirror. It is no surprise then, that the thermal gradients of the mirror clearly line up with temperature changes in the tube sensor, as seen in figure 15. When the sun begins to shine on the mirror, positive gradients form, and when the telescope faces away these gradients become negative. This is because the edges of the mirror are thinner than the center and therefore heat up and cool down more quickly. While there is certainly value to characterizing the mirror's thermal behavior during these transient conditions, the telescope tube was never intended to point directly at the sun. Unfortunately, the failure of the azimuthal motor and the shorter-than-expected flight make it difficult to validate our thermal simulations of mirror temperature in equilibrium.

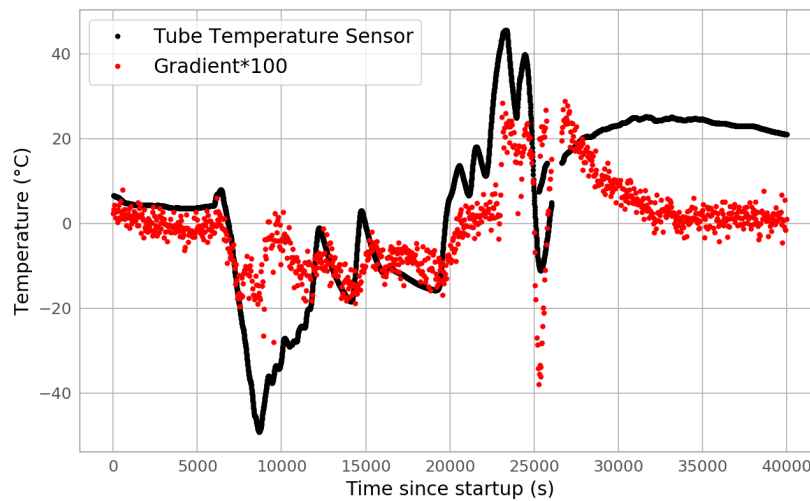


Figure 15: The gradient, multiplied by 100 for comparison, plotted with the contact sensor at the end of the telescope tube. This temperature sensor has proven to be a good indicator of the spin of the model.

5. CONCLUSIONS

Both additive and multiplicative correction greatly improve, as measured by the image standard deviation, the images taken by the Melexis 90640, but additive correction has a lesser impact on the mean and is therefore recommended for future investigations using this device. A method has been

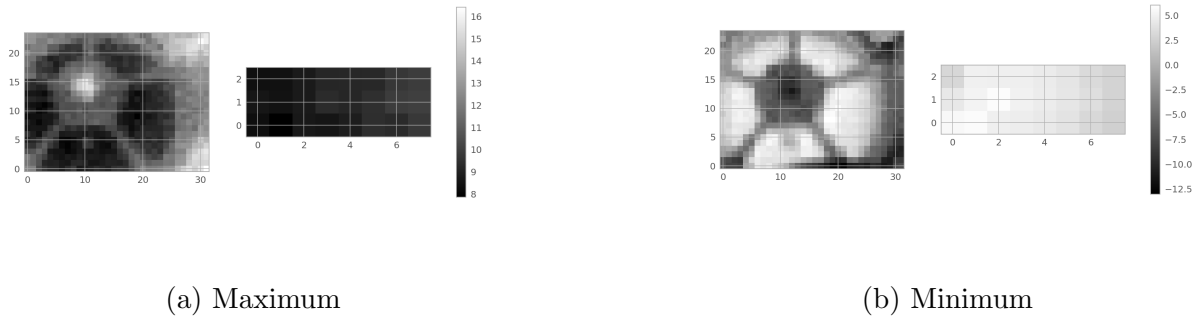


Figure 16: The maximum and minimum radial temperature gradient in the mirror occurred shorter before and during descent, respectively

developed to generate a new bias frame for any temperature from $-60^{\circ}C$ to $20^{\circ}C$. The thermal imager reports the bulk mirror temperature very closely to the contact sensor, with a small temperature offset (between $0 - 2^{\circ}C$) possibly caused by IR glow from the other, warmer, surfaces in the gondola interior. The radial temperature gradient in the mirror ranges from -0.76 to $0.58^{\circ}C/cm$ during extreme transient events such as descent. Further test flights are required to say with any certainty whether the thermal gradients in the mirror are acceptable during equilibrium conditions.

REFERENCES

- | | |
|---|--|
| <p>Young, E., Lamprecht, B., Drake, G., Smith, K., Woodruff, R., & Crotser, D. (2015), Passive thermal control of balloon-borne telescopes.</p> | <p>Brockett, G. (2015), Thermal Modeling of the High-Altitude Balloon Telescope Environment via THAI-SPICE</p> |
|---|--|